



Research article

Quantification of maternal-fetal cardiac couplings in normal and abnormal pregnancies applying high resolution joint symbolic dynamics

Ahsan H. Khandoker^{1,*}, **Haitham M. Al-Angari**¹, **Andreas Voss**², **Steffen Schulz**² and **Yoshitaka Kimura**^{3,4}

¹ Biomedical Engineering Department, Khalifa University of Science, Technology and Research, Abu Dhabi, UAE

² Institute of Innovative Health Technologies IGHT, Ernst-Abbe-Hochschule, Jena, Germany

³ Institute of International Advanced Interdisciplinary Research, Tohoku University School of Medicine, Sendai, Japan

⁴ Department of Gynecology and Obstetrics, Tohoku University Hospital, Sendai, Japan

* **Correspondence:** Email: ahsank@ieee.org; Tel: +971-2-501-8559; Fax: +971-2-447-2442.

Abstract: Maternal psycho-physiological activities affect the fetal development and its heart rate variability. In this work, the short-term maternal-fetal cardiac couplings in normal and abnormal fetuses were investigated by using the high resolution joint symbolic dynamics method. The analysis was applied on maternal and fetal beat-to-beat intervals of 66 normal and 19 abnormal fetuses that includes different types of congenital heart defects, tachycardia, Atrioventricular block and other types of abnormalities. Results showed that the weak decrease in maternal beat-to-beat variations associated with the strong increase in fetal beat-to-beat variations was found to be significantly higher for the abnormal cases compared to normal cases despite the heterogeneity of abnormality and gestational age (abnormal: 0.032 ± 0.013 , normal: 0.014 ± 0.007 , $p < 0.01$). These differences could be interpreted as impairment in the autonomic nervous system in abnormal cases. The atrioventricular block cases showed a rise in the strong increase and decrease fetal beat-to-beat variations compared to the normal cases while the tachycardia cases showed a decay in these coupling patterns.

Keywords: fetal electrocardiogram; fetal heart rate variability; maternal-fetal autonomic interaction; nonlinear coupling; joint symbolic dynamics

1. Introduction

Fetal well-being during pregnancy has been widely assessed with fluctuations of fetal heart rate or fetal heart rate variability (FHRV) monitoring. Recently there has been increasing interest in research on maternal-fetal heart rate coupling for assessing fetal health which would not be evaluated with the traditional temporal and spectral methods applied directly to fetal heart rate recordings [1]. Previous studies have shown variations in FHRV due to physiological and psychological states of the mother such as maternal stress and anxiety, exercise and low level of blood oxygen resulted in FHR changes [2–4].

Various signal processing methods were used to study the coupling between mother and fetus [1,4–7]. For example, Khandoker et al. applied normalized short time partial directed coupling (NSTPDC) to show strong influence of fetal heart rate on maternal heart rate in the early gestation [5]. This influence decreased significantly from early to mid-gestation and was associated with a significant increase of maternal to fetal coupling strength [5]. Van Leeuwen et al. have shown beat by beat synchronization between mother and fetus heartbeats by using phase synchronization [7].

The specific mechanism leading to maternal–fetal heart rate coupling remains unexplained and previous studies [7,8] proposed two hypotheses for pathways mediating this interaction: (i) the oscillatory rhythm of maternal respiration acts as a common driving force and influences simultaneously both maternal and fetal heart rates, leading to an apparent maternal–fetal heartbeat synchronization; (ii) the maternal cardiac system has a direct acoustic stimulus effect on the fetal heart rhythm.

Recently assessment of the strength's relations and their directionality of couplings have been two major aspects of investigations for a more detailed understanding of physiological regulatory mechanisms [9,10]. There are several approaches used to assess direct and indirect couplings that can be grouped into five classes basing on traditional domain classification as Granger causality, nonlinear prediction, entropy, symbolization and phase synchronization [11–16]. For nonlinear interaction analysis between heart rate, blood pressure and/ or respiratory time series the method of Joint Symbolic Dynamics (JSD, [12]) and High Resolution Joint Symbolic Dynamics (HRJSD, [17,18]) were applied. The principle of joint symbolic dynamics is to analyze nonlinear couplings between two time series based on the analysis of bivariate dynamic processes by means of symbols. Symbolization based methods enable a coarse grain quantitative assessment of short-term dynamics of time series for direct analysis of successive signal amplitudes based on discrete states (symbols) [11]. JSD quantifies coupling between two systems using two symbols: 0 and 1. Using JSD, Reulecke et al. have shown some independent heart rate regulation patterns from the respiratory regulation in quiet sleep of preterm neonates which was interpreted as an increase in the vagal modulation [19]. HRJSD was also proposed to quantify short-term cardiovascular couplings in acute schizophrenia [18]. HRJSD uses three symbols 0, 1 and 2 to characterize coupling between two systems. Schultz et al. have applied HRJSD to study baroreflex changes due to medication in a group of schizophrenia patients. They have shown an increase in the invariable BBI-E1 pattern (no variation or unchanged BBI of type 1 symbols) coupled with alternating systolic pressure (SP) families: SP-E2 (unchanged SP in type 2 patterns), SP-LU1 (one variation in three words of SP), SP-P (three variations in SP) in medicated schizophrenia patients compared to unmedicated patients. This was interpreted as impairment of the baroreflex feedback loop (which is parasympathetic) due to the anti-cholinergic effect of the antipsychotics [18].

In our previous study, HRJSD was used to study gestational age effect on healthy maternal-fetus coupling. The observed diminished fluctuating and alternating fetal heart rate patterns and intensified fast and strong fetal heart rate changes from the first to the third trimester could be an indicator of more matured adaptation of autonomic nervous system (ANS) to strong short-term maternal heart rate changes as external stimuli [20].

In this study, HRJSD method was applied to study short-term maternal-fetal cardiac couplings in abnormal cases (diseased mothers) and compare them to the healthy cases (normal pregnancies). The aim was to evaluate whether HRJSD could work as a noninvasive measure for screening fetal cardiac anomalies at an early stage.

2. Materials and method

2.1. Subjects

Recording of the maternal and abdominal ECG signals (mECG and abECG) from 85 pregnant women at the gestational age of 16~41 weeks were collected from Tohoku University Hospital. Among these cases, 66 were normal single pregnancies and 19 were abnormal pregnancies with different types of abnormality (GAa (19-38 weeks)). The normal cases were divided into three gestational age groups: GA1 (16–25 weeks), GA2 (26–30 weeks) and GA3 (32–40 weeks) and each of the groups has 22 subjects. The abnormal group has variety of abnormality such as: bradycardia, tachycardia, premature atrial contraction and different types of congenital heart defects (CHD) or anomalies (ventriculoseptal defect (VSD), atrial septal defect (ASD), pulmonary atresia (PA), tetralogy of Fallot (TOF) and Ebstein anomaly). Tables 1, 2 show demographics of the normal and abnormal cases. The study protocol was approved by Tohoku University Institutional Review Board and written informed consent were obtained from all subjects.

2.2. Data preprocessing

All recordings (each of 1 minute's length) were sampled at 1000 Hz with 16-bit resolution. Fetal ECG (fECG) traces were extracted using a method that combines cancellation of the mother's ECG signal and the blind source separation with reference (BSSR) as described in our earlier study [21]. Intervals between successive R waves of the QRS complex (i.e., R-R intervals in seconds) were calculated using the algorithm developed by Pan and Tompkins [22]. Two beat-to-beat intervals (BBI) time series namely fetal heart rates (fBBI) and maternal heart rates (mBBI) were extracted from R-R intervals of mECG and fECG signals. Both time series were visually inspected and if appropriate reedited. Afterwards these time series (fBBI, mBBI) were subsequently filtered by an adaptive filter algorithm to remove and interpolate ventricular premature beats and artefacts to obtain normal-to-normal beat time series. For the maternal-fetal coupling analyses the filtered fBBI and filtered mBBI time series were resampled (spline interpolation) using frequency $f_s = 5\text{Hz}$.

2.3. High resolution joint symbolic dynamics (HRJSD)

HRJSD was developed to analyze nonlinear cardiovascular couplings in acute schizophrenia patients based on the analysis of dynamic processes by using symbols [18]. In this study we used

HRJSD for quantifying the fetal-maternal heart rate couplings. Therefore, both time series (fBBI and mBBI) were transformed into symbol sequences. If X is a bivariate signal vector, x_n^{fBBI} and x_n^{mBBI} respectively.

$$X = \left[x_n^{fBBI}, x_n^{mBBI} \right]^T \quad n = 0, 1, 2, \dots \quad x \in R \quad (1)$$

X is then transformed into a bivariate symbol vector S which defined as

$$S = \left[S_n^{fBBI}, S_n^{mBBI} \right]^T \quad n = 0, 1, 2, \dots \quad s \in 0, 1, 2 \quad (2)$$

The definitions of symbols are as follows:

$$S_n^{fBBI} = \begin{cases} 0 & \text{if } (x_{n+1}^{fBBI} - x_n^{fBBI}) < -l^{fBBI} \\ 1 & \text{if } -l^{fBBI} \leq (x_{n+1}^{fBBI} - x_n^{fBBI}) \leq l^{fBBI} \\ 2 & \text{if } (x_{n+1}^{fBBI} - x_n^{fBBI}) > l^{fBBI} \end{cases} \quad (3)$$

similarly

$$S_n^{mBBI} = \begin{cases} 0 & \text{if } (x_{n+1}^{mBBI} - x_n^{mBBI}) < -l^{mBBI} \\ 1 & \text{if } -l^{mBBI} \leq (x_{n+1}^{mBBI} - x_n^{mBBI}) \leq l^{mBBI} \\ 2 & \text{if } (x_{n+1}^{mBBI} - x_n^{mBBI}) > l^{mBBI} \end{cases} \quad (4)$$

and the threshold levels l^{fBBI} and l^{mBBI} were considered to be 0. Symbol sequences with increasing values were coded as “2”, decreasing values were coded as “0” and unchanging (no variability) values were coded as “1”. The symbol vector S was subdivided into short words (bin) w_k of word length $k = 3$. Thus, using three symbols led to 27 different word types for fBBI (w_{fBBI}) and mBBI (w_{mBBI}) were formed and total of number of all word type combination were $729 = 27 \times 27$. Then all single word types $w_{fBBI, mBBI}$ were grouped into 8 pattern families' w_f whereby the probabilities of all single word family's occurrences $p(w_f)$ was normalized to 1. There were 8 pattern families ($E0, E1, E2, LU1, LD1, LA1, P, V$) which represent different aspects of autonomic modulation and were sorted into an 8x8 pattern family density matrix Wf resulting in 64 maternal-fetal coupling patterns. The pattern definitions are shown in Table 3 and the effects on the BBI are shown in Table 4. Additionally, the sum of each ($n = 8$) column cf_{mBBI} , the sum of each ($n = 8$) row cf_{fBBI} and the Shannon entropy ($HRJSD_{shannon}$) of Wf were calculated from the matrix Wf as a measure of overall complexity of fetal maternal coupling.

2.4. Statistics

In this study the nonparametric Mann-Whitney U-test was performed to check the differences between the normal and abnormal groups. Significances were considered for values of $p < 0.05$. All results were presented as mean \pm SD. Due to their limited numbers, qualitative comparisons were also made between some abnormality types (such as AV block and tachycardia) and the normal fetuses.

3. Results

3.1. Normal pregnancies

Figure 1 show a 3D bar plot of averaged pattern family density matrix Wf for the three normal groups and some abnormal cases. The coupling patterns between maternal and fetal time series were consistent for all three normal gestational age groups but with different strength. For example, GA1 has higher probability of occurrence; $p(w_f)$ for mBBI-E0/fBBI-LD1, mBBI-E0/fBBI-LU1 and mBBI-E2/fBBI-LD1 than GA2 and GA3 (Figure 1a–c). On the other hand, GA2 and GA3 showed higher $p(w_f)$ for mBBI-E0/fBBI-E0 and mBBI-E2/fBBI-E0 than GA1 (it was statistically significant for GA3 only). The E1, P and V patterns were completely absent in both mBBI and fBBI time series for GA1, GA2, and GA3. The significant coupling patterns between the three groups was reported in our previous work (Table 5)[20]. No significant differences were found between GA2 and GA3 which indicates that these coupling patterns do not capture changes in the development of the ANS between middle and late gestational weeks. Coupling between fetal E0 and maternal E0, E2 and LD1 patterns was significantly higher in late groups (GA3) compared to GA1, while coupling between fetal LA1 and maternal E0, LU1 and LD1 and between fetal LD1 and maternal E2 and LU1 was significantly lower for late groups (GA3).

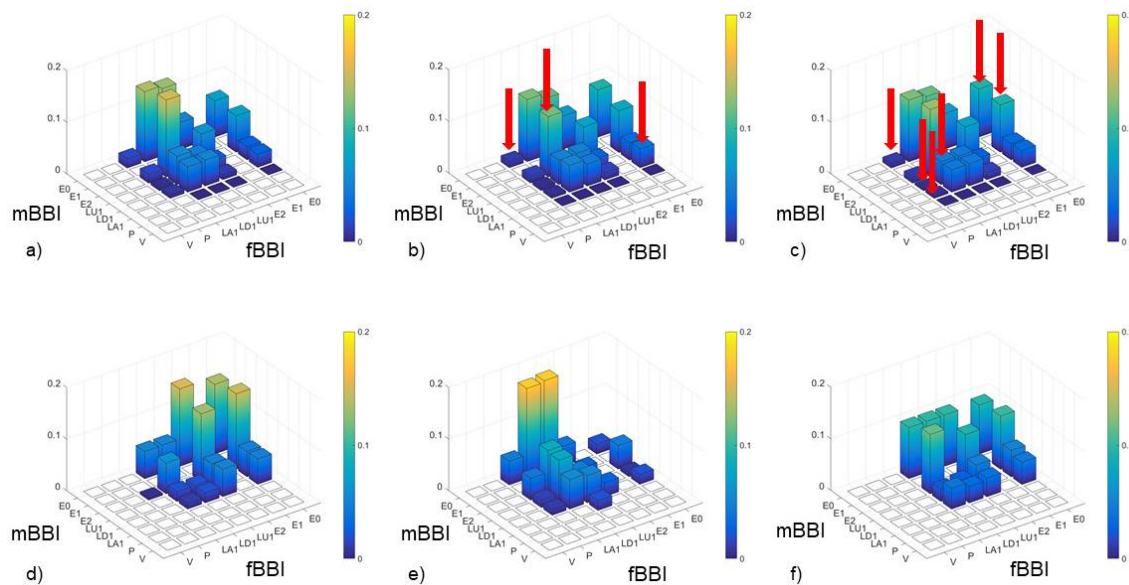


Figure 1. 3D bar plots of the mean HRJSD pattern family distribution density matrix Wf (8×8) for (a) GA1 group (b) GA2 group, (c) GA3 group, (d) an AV case, (e) a Tachycardia case and (f) a SSS case. (mBBI: maternal beat-to-beat intervals, fBBI: fetal beat-to-beat intervals). Red arrows indicate significantly different probability of occurrence from the early gestation group (GA1), $p < 0.01$.

3.2. Normal pregnancies vs. abnormal pregnancies

For the abnormal cases (AV block) revealed higher $p(w_f)$ for fetal patterns E0 and E2 (fBBI-E0,

fBBI-E2), and lower $p(w_f)$ for fetal patterns LU1 and LD1 (fBBI-LU1, fBBI-LD1) with mBBI-E0, E2, LU1 and LD1 maternal patterns than all normal groups. The fetal pattern LA1 (fBBI-LA1) diminished with the exception in combination with mBBI-E2 (Figure 1-d).

For the tachycardia case (Figure 1-e), $p(w_f)$ for the maternal patterns (mBBI-E0, E2, LU1, and LD1) coupled with the fetal pattern fBBI-E0 were lower, and were higher coupled with fBBI-LA1 in comparison to the normal cases. Also, $p(w_f)$ for mBBI-E0/fBBI-LU1 and mBBI-E0/fBBI-LD1 were higher for tachycardia case than normal ones.

For SSS cases the mBBI-LA1 and fBBI-LA1 patterns were completely absent. The mBBI-E0 pattern revealed almost equal probability of occurrence with the corresponding fetal patterns (fBBI-E0, E2, LU1 and LD1 (Figure 1-f).

Figure 2 shows plots of some coupling patterns for the normal and the abnormal cases versus gestational age. The two single-atrium/AV block cases (ID 8, 17) revealed higher probability of occurrence for the patterns mBBI-E0/fBBI-E2 and lower probability of occurrence for the patterns mBBI-E2/fBBI-LA1 than the normal cases (Figure 2-a, b). The two tachycardia cases (ID 6, 13) showed a contrary behavior in respect to the probability of occurrence of the patterns, i.e., lower probability of occurrence of the pattern mBBI-E0/fBBI-E2 and higher probability of occurrence of the pattern mBBI-E2/fBBI-LA1.

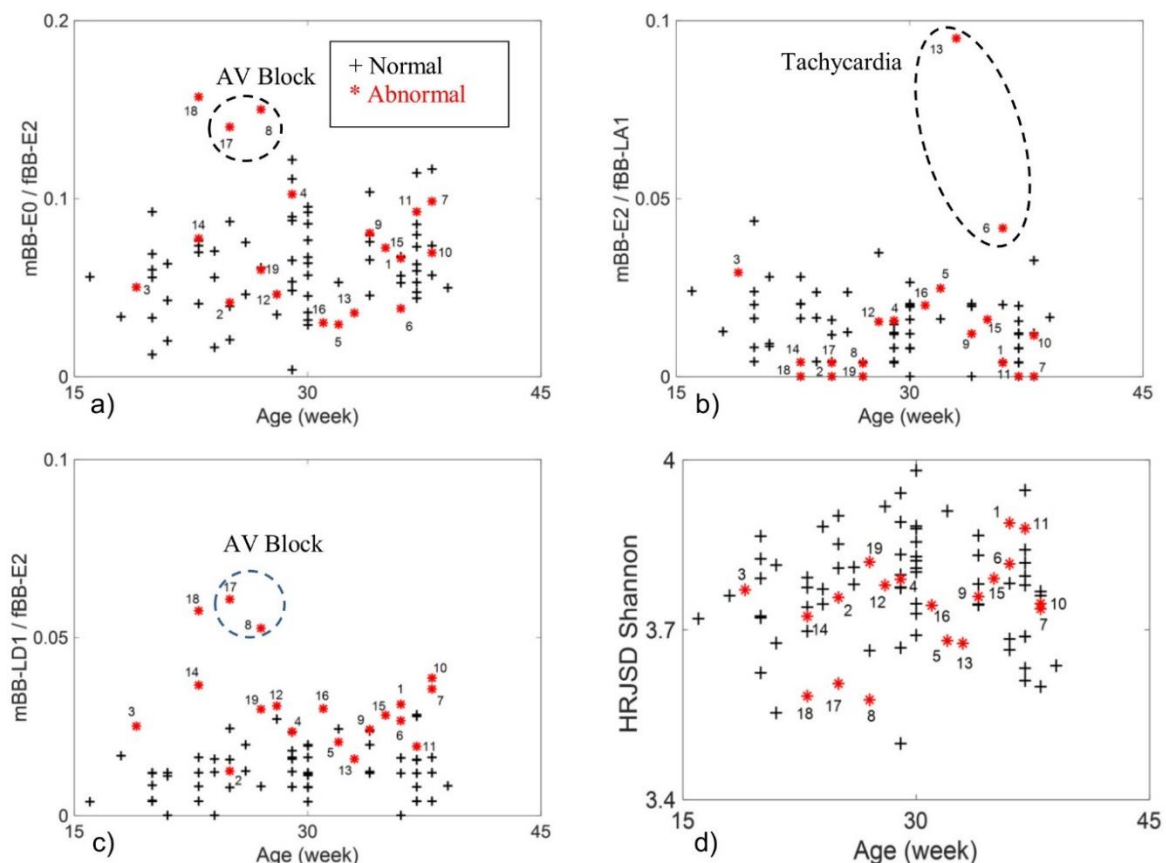


Figure 2. Examples of coupling pattern versus gestational age for normal cases vs. abnormal cases. (a) mBBI-E0/fBBI-E2, (b) mBBI-E2/fBBI-LA1, (c) mBBI-LD1/fBBI-E2, (d) HRJSD Shannon entropy.

Table 1. Demographic data for the normal fetuses.

Group	Gestational weeks	Maternal age (years)	Maternal BMI	EFBW	Gravida	Para
GA1 (n = 22)	21.8 ± 2.4	31.1 ± 3.4	22.6 ± 2.6	654.4 ± 248.9†	1.6 ± 1.0	0.7 ± 1.0
GA2 (n = 22)	29.0 ± 1.3	30.6 ± 3.1	23.0 ± 3.1	1285 ± 291.7*	1.2 ± 0.8	0.4 ± 0.5
GA3 (n = 22)	36.2 ± 1.8	29.9 ± 6.2	22.6 ± 6.1	2571 ± 308.8*,†	0.7 ± 0.8*	0.1 ± 0.3*

EFBW: Estimated Fetal Birth Weight. Gravida: number of pregnancy times. Para: number of pregnancies reach viable gestational age (*: significantly different from GA1, †: significantly different from GA2, p < 0.05).

Table 2. Demographics of the abnormal cases.

ID	GA	Maternal age (years)	Maternal BMI	EFBW	Para	Gravida	Delivery mode	Abnormality
1	36	24	23.1	2373	1	1		WPW
2	25	34	36.2	449	0	0	C-section	Placental dysfunction
3	19	-	-	-	-	-	-	TTTS Donner
4	29	30	22.8	-	-	-	-	hydrops fetalis
5	31	30	21.8	-	-	3	-	Medical history of intrauterine fetal death
6	36	34	21.1	2448	1	1	Natural	Fetal Tachycardia
7	38	44	23.4	-	-	-	-	SSS
8	27	-	-	-	-	-	-	AV Block, CHD, SA, CAV
9	34	23	22.1	2600	0	0	Emergency C-section	Cardiac dilatation, CHD
10	38	26	23.6	-	0	0	C-section	PAC, IUGR
11	37	-	-	-	-	-	-	CHD
12	28	41	22.9	859	1	0	-	TOF, VSD, PA, MS, PAC
13	33	28	25.5	-	-	-	-	Fetal Tachycardia
14	23	36	21.5	-	-	3	-	CHD
15	35	32	-	2100	1	1	-	CHD
16	31	37	21.5	1157	-	-	-	Heart Failure
17	25	41	36.2	767	1	1	-	PA, CAVC, SA, AV Block, Polysplenia syndrome
18	23	25	22.1	-	-	-	-	VSD, ASD, CDH, Chromosomal aberration
19	27	25	22.9	1332	0	0	stillbirth	Ebstein syndrome

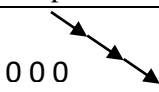
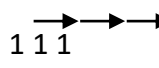
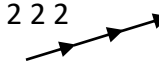
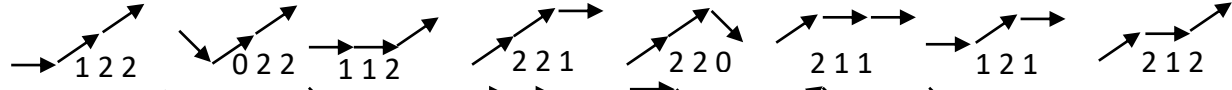
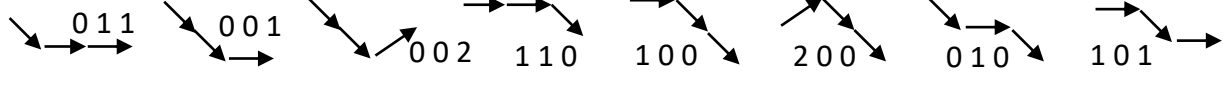
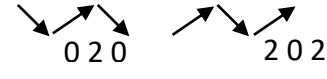
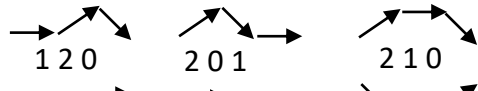
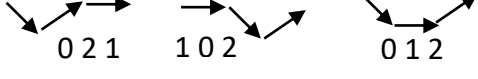
GA: gestational age in weeks. EFBW: Estimated Fetal Birth Weight. Gravida: number of pregnancy times. Para: number of pregnancies reach viable gestational age. Abnormality abbreviations: 1) WPW: Wolff–Parkinson–White syndrome, 2) TTTS: twin-twin transfusion syndrome, 3) SSS: sick sinus syndrome, 4) CHD: congenital heart defect, 5) SA: single atrium, 6) CAV: cardiac allograft vasculopathy, 7) PAC: premature atrial contraction, 8) IUGR: intrauterine growth restriction, 9) TOF: tetralogy of Fallot, 10) VSD: ventriculoseptal defect, 11) PA: pulmonary atresia, 12) MS: mitral stenosis, 13) CAVC: common atrioventricular canal, 14) ASD: atrial septal defect, 15) CDH: congenital diaphragmatic hernia.

Table 3. Definition of the 8-pattern families of HRJSD.

E0	No variation in the word that consists of three symbols of the type '0' ('000': decreasing BBI)
E1	No variation in the word that consists of three symbols of the type '1' ('111': unchanged BBI)
E2	No variation in the word that consists of three symbols of the type '2' ('222': increasing BBI)
LU1	One variation in the word that consists of two different symbols with low increasing behavior of BBI ('122', '022', '112', '221', '220', '211', '121', '212')
LD1	One variation in the word that consists of two different symbols with low decreasing behavior of BBI ('011', '001', '002', '110', '100', '200', '010', '101')
LA1	One variation in the word that consists of two different alternating symbols of type '0' and '2' with an increasing-decreasing behavior of BBI ('020', '202')
P	Three variations in the word that consists of three different symbols with peak-like behavior ('120', '201', '210')
V	Three variations in the word that consists of three different symbols with valley-like behavior ('021', '102', '012')

BBI: beat-to-beat intervals.

Table 4. Effect of pattern families on successive BBI.

Pattern	Description
E0	
E1	
E2	
LU1	
LD1	
LA1	
P	
V	

Interestingly, the mBBI-LD1/fBBI-E2 pattern was the only HRJSD maternal-fetal coupling pattern that was significantly higher for the all abnormal cases (GAa) compared to normal cases (GA) despite the heterogeneity of abnormality ones (GAa: 0.032 ± 0.013 , GA: 0.014 ± 0.007 , $p < 0.01$ Figure 2-c). The HRJSD_{Shannon} entropy was significantly higher for the normal cases (GAa: 3.5 ± 0.09 , GA: 3.6 ± 0.14 , $p < 0.05$ Figure 2-d). The significant measures between GAa and GA groups are summarized in Table (6).

Table 5. Significant HRJSD indices from maternal fetal cardiac coupling analysis (*: significantly different from GA1 group, $p < 0.01$) among three groups (GA1(16-25 weeks) early fetus; GA2 (26-30 weeks) and GA3 (32-41 weeks)).

Index	GA1 (n = 22)	GA2 (n = 22)	GA3 (n = 22)
mBBI-E0/fBBI-E0	7.0 ± 2.5	9.2 ± 3.7	9.3 ± 2.3*
mBBI-E0/fBBI-E2	5.2 ± 2.3	6.6 ± 2.8	6.9 ± 2.1
mBBI-E0/fBBI-LU1	13.0 ± 2.4	11.0 ± 3.0	11.4 ± 2.4
mBBI-E0/fBBI-LD1	13.6 ± 1.7	11.9 ± 2.4	12.0 ± 2.3
mBBI-E0/fBBI-LA1	1.8 ± 0.8	1.1 ± 0.7*	1.0 ± 0.7*
mBBI-E2/fBBI-E0	7.0 ± 1.8	8.2 ± 3.2	9.2 ± 2.9*
mBBI-E2/fBBI-E2	6.0 ± 1.9	7.3 ± 2.8	7.3 ± 2.3
mBBI-E2/fBBI-LD1	14.9 ± 2.5	11.4 ± 3.0*	13.1 ± 2.2
mBBI-E2/fBBI-LA1	1.7 ± 1.0	1.3 ± 0.8	1.2 ± 0.9
mBBI-LU1/fBBI-E0	2.6 ± 1.0	3.3 ± 1.3	3.2 ± 1.2
mBBI-LU1/fBBI-LD1	5.5 ± 1.4	4.9 ± 1.9	4.4 ± 1.3*
mBBI-LU1/fBBI-LA1	0.6 ± 0.3	0.5 ± 0.4	0.3 ± 0.4*
mBBI-LD1/fBBI-E0	2.6 ± 0.8	3.8 ± 1.5*	3.3 ± 1.0
mBBI-LD1/fBBI-LA1	0.7 ± 0.4	0.5 ± 0.4	0.3 ± 0.5*
mBBI-LA1/fBBI-LA1	0.0 ± 0.0	0.1 ± 0.2	0.0 ± 0.1
fBBI-E0	16.8 ± 3.7	21.9 ± 5.9*	21.9 ± 4.4*
fBBI-E2	12.6 ± 2.7	16.0 ± 4.2*	16.1 ± 3.7*
fBBI-LD1	33.8 ± 2.7	29.7 ± 4.6*	29.7 ± 3.3*
fBBI-LA1	4.1 ± 1.2	3.1 ± 1.5	2.5 ± 1.4*

Table 6. Significant HRJSD indices from maternal fetal cardiac coupling analysis the normal group (GA) and the abnormal group (GAa).

Index	GA (n = 66)	GAa (n = 19)
mBBI-LD1/fBBI-E2*	0.014 ± 0.007	0.032 ± 0.013
HRJSD _{Shannon} **	3.6 ± 0.14	3.5 ± 0.09

(*: $p < 0.01$, **: $p < 0.05$)

4. Discussion

4.1. Normal pregnancies

The normal maternal-fetal cardiac coupling was mainly characterized by diminished fluctuating and alternating fetal heart rate patterns (fBBI-LD1 and fBBI-LA1) from the first to the third trimester whereas fast and strong fetal heart rate changes (fBBI-E0 and fBBI-E2) were intensified from the first to the end of the third trimester. It seems that the fetal heart rate gets more synchronized with the maternal heart rate as a stimulus from the beginning of the first trimester to the end of the third trimester. It could also be an indicator that the more matured adaptation of autonomic nervous system (ANS) causing strong short-term maternal heart rate (mBBI-E0 and mBBI-E2) changes as external stimuli taking place much faster at the end of the third trimester than in the beginning of the first

trimester. Furthermore, ANS maturation for regulating fetal heart rate changes seem to take place in the first two trimesters. Based on previous study, fetal ANS starts to develop in the 17th gestational week where the parasympathetic nerves develop rapidly in the 18th gestational week while development of the sympathetic nerves begins around the 20th gestational week, later than does that of the parasympathetic nerves, and is most rapid during the 26th to 30th gestational weeks [23].

4.2. Normal pregnancies vs. abnormal pregnancies

For the abnormal cases, some types of abnormality (particular conduction abnormalities) showed increase and some showed decrease in different maternal-fetal coupling patterns than the normal (GA) and the other types of abnormal cases. For example, the single atrium/AV-block cases showed a higher probability of occurrence of the patterns characterized by strong fetal heart rate increases and decreases (fBBI-E0 and E2) and a lower probability of occurrence of the patterns characterized by more variations (fBBI-LU1, LD1 and LA1). This might indicate the continuous elongation of the P-R interval (of the ECG) during the AV block [24].

For the tachycardia cases, a higher probability of occurrence for the patterns representing weak fetal heart rate alternation (fBBI-LA1) and a lower probability of occurrence of the patterns representing strong fetal heart rate increases (fBBI-E0) and decreases (fBBI-E2). This could have happened due to an increase in the vagal tone manifested by an increase in the beat-to-beat variability (the rmssd for the two tachycardia was 12 and 19 ms while it was 2.8 ± 1.3 ms for the normal GA group). This could be speculated as an autonomic reflex to halt the tachycardia similar to the known vagal maneuver that is used to slow down heart rate [25].

Despite the type of abnormality, abnormal cases tended to have higher association (probability of occurrence) between maternal slow heart rate variations and fetal heart rate strong decrease (mBBI-LD1/fBBI-E2) than normal cases. This might be indicating an imbalance in ANS adaption/modulation and could be a good marker for screening fetal cardiac wellbeing throughout the weeks of pregnancy. Measuring the degree of this coupling for developing fetuses may be useful clinical markers of healthy prenatal development and fetal cardiac anomalies. Further investigations are needed to clarify the physiological significance of the maternal–fetal heart rate coupling, and whether fetus can benefit from this specific interaction.

5. Conclusion

HRJSD method has shown variation in coupling patterns strength that reflects the development of normal fetuses during the pregnancy period. It has also shown differences between normal and abnormal fetuses in certain coupling patterns. Further analysis with more cases of similar abnormality cases is needed to assess the accuracy of HRJSD in detecting/screening certain types of fetal abnormality by using fetal and maternal HRV.

Author contributions

AHK, SS and AV designed the study. YK collected the maternal and fetal ECG data. SS and AV applied signal processing methods and extracted coupling features. SS and HMA ran statistical analysis on results. AHK, SS, HMA and AV evaluated results of the statistical analysis. HMA wrote

the main manuscript text and prepared the tables and figures and SS revised them. All authors reviewed the manuscript.

Approval, accordance and informed consent

The study protocol was approved by Tohoku University Institutional Review Board (IRB: 2015-2-80-1) and written informed consent was obtained from all subjects. All experiments were performed in accordance with relevant guidelines and regulations.

Data availability

Data used in this study will be made available upon request because we did not have any approval from ethics committee to make the data publicly available. The pregnant mothers recruited for this study did not give consent to make their data and signals available in the public domain. However, the following persons can be contacted to obtain the data under a confidentiality agreement. Dr Ahsan Khandoker (ahsan.khandoker@kustar.ac.ae); Dr Yoshitaka Kimura (ykimura@med.tohoku.ac.jp).

Conflict of interest

The authors declare no competing interests.

Funding

This study was supported by research incentive funds from Khalifa University Internal Research Fund (CIRA-2019-023).

References

1. A. H. Khandoker, S. Schulz, H. M. Al-Angari, et al, Alterations in maternal-fetal heart rate coupling strength and directions in abnormal fetuses, *Front. Physiol.*, **10** (2019), 482.
2. C. Monk, W. P. Fifer, M. M. Myers, et al, Maternal stress responses and anxiety during pregnancy: Effects on fetal heart rate, *Dev. Psychobiol.*, **36** (2000), 67–77.
3. D. J. Bekedam, E. J. Mulder, R. J. Snijders, et al, The effects of maternal hyperoxia on fetal breathing movements, body movements and heart rate variation in growth retarded fetuses, *Early Hum. Dev.*, **27** (1991), 223–232.
4. P. Van Leeuwen, K. M. Gustafson, D. Cysarz, et al, Aerobic exercise during pregnancy and presence of fetal-maternal heart rate synchronization, *PLoS One*, **9** (2014), e106036.
5. A. H. Khandoker, F. Marzbanrad, A. Voss, et al, Analysis of maternal-fetal heart rate coupling directions with partial directed coherence, *Biomed. Signal. Proces.*, **3** (2016), 25–30.
6. M. Riedl, P. Van Leeuwen, A. Suhrbier, et al, Testing foetal-maternal heart rate synchronization via model-based analyses, *Phil. Trans. Math. Phys. Eng. Sci.*, **367** (2009), 1407–1421.
7. P. Van Leeuwen, D. Geue, M. Thiel, et al, Influence of paced maternal breathing on fetal-maternal heart rate coordination, *Proc. Natl. Acad. Sci. U S A*, **106** (2009), 13661–13666.

8. P. Ivanov, Q. D. Ma, R. P. Bartsch, Maternal-fetal heartbeat phase synchronization, *Proc. Natl. Acad. Sci. U S A*, **106** (2009), 13641–13642.
9. A. Porta and L. Faes, Assessing causality in brain dynamics and cardiovascular control, *Phil. Trans. Math. Phys. Eng. Sci.*, **371**(2013), 20120517.
10. S. Schulz and A. Voss, Cardiovascular and cardiorespiratory coupling analysis—State of the art and future perspectives, in *Cardiovascular Oscillations (ESGCO), 2014 8th Conference of the European Study Group*, (2014), 25–26.
11. S. Schulz, F. C. Adochiei, I. R. Edu, et al, Cardiovascular and cardiorespiratory coupling analyses: A review, *Phil. Trans. Math. Phys. Eng. Sci.*, **371**(2013): 20120191.
12. M. Baumert, T. Walther, J. Hopfe, et al, Joint symbolic dynamic analysis of beat-to-beat interactions of heart rate and systolic blood pressure in normal pregnancy, *Med. Biol. Eng. Comput.*, **40** (2002), 241–245.
13. L. Faes, A. Porta and G. Nollo, Mutual nonlinear prediction as a tool to evaluate coupling strength and directionality in bivariate time series: comparison among different strategies based on k nearest neighbors, *Phys. Rev. E, Stat. nonlin. Soft Matter phys.*, **78** (2008): 026201.
14. A. Porta, G. Baselli, F. Lombardi, et al, Conditional entropy approach for the evaluation of the coupling strength, *Biol. Cybern.*, **81** (1999), 119–129.
15. M. G. Rosenblum and A. S. Pikovsky, Detecting direction of coupling in interacting oscillators, *Phys. Rev. E Stat. nonlin. Soft Matter phys.*, **64** (2001), 045202.
16. T. Milde, K. Schwab, M. Walther, et al, Time-variant partial directed coherence in analysis of the cardiovascular system, A methodological study, *Physiol. Meas.*, **32** (2011), 1787–1805.
17. S. Schulz, J. Haueisen, K. J. Bar, et al, High-resolution joint symbolic analysis to enhance classification of the cardiorespiratory system in patients with schizophrenia and their relatives, *Phil. Trans. Math. Phys. Eng. Sci.*, **373** (2015), 2034.
18. S. Schulz, N. Tupaika, S. Berger, et al, Cardiovascular coupling analysis with high-resolution joint symbolic dynamics in patients suffering from acute schizophrenia, *Physiol. Meas.*, **34** (2013), 883–901.
19. S. Reulecke, S. Schulz and A. Voss, Autonomic regulation during quiet and active sleep states in very preterm neonates, *Front. Physiol.*, **3** (2012), 61.
20. A. H. Khandoker, S. Schulz, Y. Kimura, et al, Investigating maternal-fetal heart rate coupling by high resolution joint symbolic dynamics, *Comput. Cardiol.*, **41** (2014), 441–444.
21. M. Sato, Y. Kimura, S. Chida, et al, A novel extraction method of fetal electrocardiogram from the composite abdominal signal, *IEEE Trans. Biomed. Eng.*, **54** (2007), 49–58.
22. J. Pan and W. J. Tompkins, A Real-Time Qrs Detection Algorithm, *IEEE Trans. Biomed. Eng.*, **32** (1985), 230–236.
23. T. Ohta, K. Okamura, Y. Kimura, et al, Alteration in the low-frequency domain in power spectral analysis of fetal heart beat fluctuations, *Fetal Diagn. Ther.*, **14** (1999), 92–97.
24. Types of Heart Block, 2012. Available from: www.nhlbi.nih.gov/health/health-topics/topics/hb/types.
25. S. H. Lim, V. Anantharaman, W. S. Teo, et al, Comparison of treatment of supraventricular tachycardia by Valsalva maneuver and carotid sinus massage, *Ann. Emerg. Med.*, **31** (1998), 30–35.

